Supporting information for

Novel precipitated zirconia-based DGT technique for high-resolution imaging of oxyanions in waters and sediments

Dong-Xing Guan[1], Paul N. Williams[2], Jun Luo[1]*, Jian-Lun Zheng[1], Hua-Cheng Xu[3], Chao Cai[4], and Lena Q. Ma[1,5]

[1] State Key Laboratory of Pollution Control and Resource Reuse, School of the Environment, Nanjing University, Jiangsu 210023, China

[2] Institute for Global Food Security, School of Biological Sciences, Queen's University Belfast, Belfast BT9 7BL, United Kingdom

[3] State Key Laboratory of Lake Science and Environment, Nanjing Institute of Geography and Limnology, Chinese Academy of Sciences, Nanjing 210008, China

[4] Institute of Urban Environment, Chinese Academy of Sciences, Xiamen 361021, China

[5] Soil and Water Science Department, University of Florida, Gainesville, FL 32611, USA

* Corresponding authors, 0086–25–89680632, esluojun@nju.edu.cn

CONTENTS

Table S13. Elution efficiencies of As and Se from precipitated zirconia gels eluted using different volumes and concentrations of NaOH. Standard deviations are derived from replicates (n=6).

Table S14. Diffusive coefficients adopted in this study.

Table S15. The ratio of concentrations of elements measured by DGT containing precipitated zirconia gels to concentrations in solutions with different concentration ratios for P, V, As, Se, Mo and Sb. Standard deviations are derived from replicates (n=3).

Figure S1: Scheme of the mescosm experimental design.

Figure S2: Masses of P, V, As, Se, and Sb bound onto precipitated zirconia gels. The gels were soaked in solutions containing 200 μg L^{-1} P or 100 μg L^{-1} V, As, Se, or Sb for different deployment time. Error bars represent the standard deviations of replicates (n=3).

Figure S3: Temporal change of each three precipitated zirconia (PZ) and slurry zirconia (SZ) gels discs of circular shape before and after gel drying. Discs marked PZ gel were PZ gel discs, and the left were SZ gel discs.

Figure S4: Temporal change of each three precipitated zirconia (PZ) and slurry zirconia (SZ) gels discs of quadrangular shape before and after gel drying. FM represented filter membrane.

Figure S5: SEM images of precipitated zirconia gel. Scale at 10 μm (up) and 1 μm (down).

Figure S6: Vertical pH profile in the upper 4.4 mm of the sediment with a resolution of 50 μm.

Figure S7. Principal component analysis (PCA) of fluxes of P, As, Mo and Sb in four discrete zones. The size of each zone is 1200 μm × 3000 μm containing 240 points, i.e. n=240.

Figure S8: Percentages of As (a) and Sb (b) species during 24 h stirring of 2 L of 100 μg L^{-1} AsIII or SbIII with a matrix of 0.01 mol L^{-1} $NaNO_3$. Solid and open columns represent reduction(III) and oxidation(V) state, repectively, of As and Sb. C-1, C-2, C-3 and C-4 indicate the controls of As and Sb solutions without stirring.

Figure S9. Recovery of P from precipitated zirconia gels eluted using 10 ml of different concentrations of NaOH solution. The solid line shows the 95% recovery of P. Error bars represent the standard deviations of replicates (n=6).

Figure S10. Dependence of measured mass of P, V, As, Se, Mo and Sb accumulated by DGT equipped with precipitated zirconia gels on different deployment time (from 4 to 72 h). The solid lines were calculated from independently measured solution concentrations using equation S4. Error bars represent the standard deviations of replicates (n=3).

Figure S11. Dependence of the measured mass of P, V, As, Se, Mo and Sb accumulated by DGT devices containing precipitated zirconia gels on the reciprocal of diffusive gel thicknesses (4 h deployment). The solid lines were calculated from independently measured solution concentrations using equation S4. Error bars represent the standard deviations of replicates (n=3).

PRINCIPLES OF DGT

Diffusive gradients in thin films (DGT) is a passive sampling technique which is based on Fick's first law of diffusion (Equation S1). DGT devices consist of a binding gel layer, an ion-permeable diffusive gel layer, an overlying protective filter membrane and a plastic base and cap that holds all the layers tightly together.[1] Ions diffuse through the well-defined diffusive layer and filter membrane, and formed a linear steady state concentration gradient. Afterwards, the ions are immediately bound onto a binding layer, which results in an effective zero concentration at the diffusive and binding layer interface.

According to Fick's first law, the flux (F) of an ion through the diffusive gel and filter can be expressed as (Equation S1).

$$F = D\frac{\partial C}{\partial x} = D\frac{(\mathrm{C}-\mathrm{C}')}{\Delta g} \quad \text{(S1)}$$

Where D is the diffusion coefficient of an ion in the diffusive gel and filter membrane, $\partial C/\partial x$ is the concentration gradient, C is the ion concentration in the solution, C', the concentration of the ion at the interface of binding layer and diffusive layer, and Δg is the thickness of the diffusive gel and filter membrane. Before the binding layer reaches saturated, C' equals to zero. Then equation S1 becomes S2.

$$F = D\frac{C}{\Delta g} \quad \text{(S2).}$$

Flux, F, can also be expressed as equation S3.

$$F = \frac{M}{t} \quad \text{(S3)}$$

Where M is mass of an ion diffusing through an area (A) in a given time (t).

Combing equation S2 and S3 can get equation S4.

$$C = \frac{M\Delta g}{DAt} \quad \text{(S4)}$$

The total mass (M) of accumulated ions on the binding layer is usually measured after elution by appropriate reagents with known volume (V_{elute}), i.e. HNO_3, NaOH, etc. The mass of elements accumulated in the binding layer can be calculated using equation S5.

$$M = \frac{C_e(\mathrm{V}_{gel} + \mathrm{V}_{elute})}{f_e} \quad \text{(S5)}$$

Where C_e is the concentration in the eluting solution, f_e is the elution factor for an ion, V_{gel} and V_{elute} are the volume of the binding layer and eluting reagent, respecitively.

EXPERIMENTAL

Preparation of oxyanion solutions. Oxyanion solutions were prepared using KH_2PO_4, Na_3VO_4, $Na_2HAsO_4 \cdot 7H_2O$, $NaAsO_2$, $Na_2SeO_4 \cdot 10H_2O$, $Na_2SeO_3 \cdot 5H_2O$, $Na_2MoO_4 \cdot 2H_2O$, $NaSbO_3 \cdot 3H_2O$ and $C_8H_4K_2O_{12}Sb_2 \cdot 3H_2O$. All chemicals were of analytical grade or better. To avoid oxidation changes, species at lower oxidation state were measured using high performance liquid chromatography (HPLC, Waters e2695, Ireland) – inductively coupled plasma mass spectrometry (ICP–MS, PerkinElmer NexION 300X, USA), with little changes (< 5.4%) of species occurring during 24 h deployment in stirred solutions (Figure S8).

Effects of deployment time, diffusive gel thickness, competition among oxyanions on DGT performance. The effect of deployment times was tested by immersing DGT devices in 6 L of well-stirred solution containing 100 μg L^{-1} P, 50 μg L^{-1} As, Se, V, Mo, and Sb and 0.01 mol L^{-1} $NaNO_3$ up to 72 h. To assess the possible effect of diffusive gel thickness on mass accumulation of analytes by the gel, DGT devices with varied diffusive gel thickness were immersed for 24 h in 6 L of solution containing 100 μg L^{-1} P, 50 μg L^{-1} V, As, Se, Mo, and Sb and 0.01 mol L^{-1} $NaNO_3$. To study the competition effect among these six oxyanions in solutions, DGT devices with PZ gels were deployed for 4 h in 2 L well-stirred solutions containing 0.01 mol L^{-1} $NaNO_3$: (a) P at 100 μg L^{-1} and the other five elements at 500 μg L^{-1}; (b) As, Se, or Mo at 50 μg L^{-1} and other five elements at 500 μg L^{-1}; (c) V and Sb at 50 μg L^{-1} and P, As, Mo, and Se at 5 mg L^{-1}.

Preparation of AgI gels. 0.153 g silver nitrate (99.99% metal basis, Aladdin Industrial Corp., China) was dissolved in 0.45 mL of Milli-*Q* (MQ) water. 8.55 mL of gel solution[2] was well mixed with 36 μL of ammonium persulfate (APS, 5% w/w, BDH), then the dissolved $AgNO_3$ was added and well mixed in dark (from here to rinsing the gel, all the experiments were performed in dark). Following addition of $AgNO_3$, the solution was cast immediately between glass plates spaced by a 0.5 mm spacer, which is different from that of 0.25 mm spacer reported by Stockdale et al.[3] The polymerization process was performed at room temperature (20°C) in dark conditions for 1 h. Thereafter, the glass plates were opened, and one glass plate was removed, leaving the gel adhering to the other plate. The gel and plate were then immersed in 500 mL of 0.2 mol L^{-1} KI (guaranteed reagent, Aladdin industrial corporation, China). After a few minutes, the gel, turning white, was peeled off from the plate and kept in the KI solution overnight to allow full development. After being taken out from the solution, the gel was rinsed several times in MQ water to remove excess reagents, and soaked in MQ water. After hydration, a 0.8 mm-thick AgI gel was obtained, and was used as diffusive gel in the probe for sediment.

Horizontal shrinkage examination of slurry and precipitated zirconia gels during the gel drying procedure. Gel dry procedure is a prerequisite for laser ablation inductively coupled plasma mass spectrometry (LA–ICP–MS) high-resolution analysis. The procedure adopted in this paper is followed by Stockdale et al.[4] In short, there are two steps: (1) pre-drying the gel and backing filter membrane (polyethersulfone, 0.45 μm, Whatman, UK) by light pressure overnight; (2) gel drying of the pre-dried gel and filter membrane by a gel drier (Model 583, Bio-rad, USA) connected to a pump (165-1782, HydroTech^{TM} Vacuum Pump, Bio-rad, USA) at 60^{o}C (PAGE drying cycle) for 8 h. Distinguished form precipitated zirconia gel (PZ gel), slurry zirconia gel (SZ gel)[5, 6] is produced without cross-linker, then as a result some horizontal shrinkage may occur during the gel drying procedure. To check this, SZ and PZ gel discs of circular shape with diameter of ~2.48 cm were dried according to the above mentioned procedure. Diameter (d) of the gel discs before and after gel drying was measured with a ruler exact to within a millimeter. Equation S6 was used to calculate the horizontal shrinkage (area, S) caused by the gel drying process.

$S=\pi(d/2)^2$ (S6)

Since high-resolution at sub-millimeter scale can be obtained by coupling DGT with LA–ICP–MS, more accuracy is needed to check the horizontal shrinkage. Then we cut circular gel disc into quadrangular shape with two backing filter membranes using Teflon-coated razor blades. In this way, the resulting disc and membranes were of the same size. The disc and the closest backing filter membrane were thus gel dried, with the other filter membrane air dried as control. Each three quadrangular PZ and SZ gel discs were chosen for gel drying. The length of four sides of gel-dried discs and filter membranes, and also the control filter membranes were measured with a Vernier caliper exact to 0.1 mm. The horizontal shrinkage (S) was calculated according to equation S7.

$$S=\sqrt{(p-a)(p-b)(p-c)(p-d)-abcd\cos^2\varphi} \quad \text{(S7)}$$

Where, a, b, c, and d are the lengths of four sides; p=(a+b+c+d)/2; φ =(A+C)/2=(B+D)/2, A, B, C, and D are the degrees of four inner angles.

As for the quadrangles we cut, φ =(A+C)/2≈π/2, then equation S7 can be expressed as equation S8.

$$S=\sqrt{(p-a)(p-b)(p-c)(p-d)} \quad \text{(S8)}$$

Sediment sampling and treatment. Sediment sampling and treatment followed established procedures.[7] One sediment core was collected from the sampling site

(31°30'48" N-162 120°12'30" E from163 Meiliang Bay within the freshwater Lake Taihu) to a depth of 50 cm using PVC pipe (4.7 cm in diameter). The core was sealed with rubber blocks and black plastic bags immediately after being retrieved. The depth of overlaying water is ~ 10 cm. The sediment core was stored in the dark at 20±2^{o}C before DGT deployment. Before and after deployment of DGT probe, the overlying water temperature was measured. Afterwards, sediment pH, total organic carbon and particle size were analyzed.

Vertical pH profile in the sediment. The vertical pH profile in the upper 4.4 cm of the sediment was measured using a pH glass microelectrode (10 μm diameter tip, built-in reference electrode, Unisense, Denmark). The sensor was calibrated at *in situ* temperature with commercial buffers (pH 4, 6.9 and 9.2) before and after deployment. The microelectrode was mounted in a motorized micromanipulator (Unisense, Denmark) for precise positioning of the microelectrode along the *z* axis of the sediment with a resolution of 50 μm.

QA/QC. To validate the adsorption and recovery efficiencies of the oxyanions to and from the PZ gels, the SLRS-5 river water reference material was analyzed. This reference material has certified values of four of the analytes, i.e. V, As, Mo and Sb. The results as presented in Table S11 indicated that the measured concentrations were in good agreement with the certified concentrations, and confirmed the robustness of the analytical procedure.

RESULTS AND DISCUSSION

DGT blank concentrations and method detection limits. To assist clear comparison with experimental data of DGT measured in waters and sediments, DGT blank concentrations were obtained by converting the measured masses on the DGT blank gels to blank concentrations based on the assumption of a deployment time of 24 h at 25^{o}C with 0.8 mm thick diffusive gels and 3.14 cm^{2} exposure area. Method detection limits (MDLs) were calculated as three times the standard deviation of the DGT blank concentrations. DGT blanks and MDLs obtained in this study and those of previously reported slurry and precipitated ferrihydrite gels[8] and Metsorb gels[9] are shown in Table S12. They are generally comparable among DGT devices equipped with different binding gels (ferrihydrite and Metsorb gels). These comparisons suggest that DGT devices equipped with PZ gels are suitable for trace and even ultra–trace analysis of the six oxyanions in waters. When their concentrations were lower than the MDLs, a longer deployment time and thinner diffusive thickness can be used to increase the accumulated mass on the PZ gels and hence further lower the MDLs proportionately.

Elution efficiency. The elution efficiency of P was investigated by soaking PZ gels, which bound different amounts of P (from 120 to 2000 ng per disc), into 10 mL of NaOH solutions. The elution recovery of P was ~95% using 0.3 mol L^{-1} to 1.0 mol L^{-1} NaOH solution and reached the maximum at 96.2% using 0.5 mol L^{-1} NaOH concentration (Figure S9), indicating that obtained elution efficiency of P should be robust. The elution efficiency of As and Se were tested by soaking loaded PZ gels in NaOH solutions with different volumes (1, 5 or 10 mL) and concentrations (0.5 or 1.0 mol L^{-1}). The maximum recovery of As and Se were achieved at 10 mL of 0.5 mol L^{-1} NaOH (Table S13). So 10 mL of 0.5 mol L^{-1} NaOH was chosen to elute all the six oxyanions and their elution efficiencies are shown in Table S4.

Effect of deployment time, gel layer thickness and competition among oxyanions. The measured masses of oxyanions, accumulated by DGT with PZ gels, increased linearly with deployment time (t) over 72 h (Figure S10) and were proportional to the reciprocal of the diffusive gel thicknesses (1/Δg) (Figure S11). The function of mass versus t or 1/Δg concurs with previous work for either one or several oxyanions measured by DGT with slurry ferrihydrite[10], precipitated ferrihydrite[8], Metsorb[9] and SZ gels[6]. Good agreement between DGT measurement and theoretical prediction, not only confirms the role of PZ gels acting as an infinite sink, but also supports the values of the adopted diffusive coefficients (Table S14) in this study.

DGT devices containing PZ gels were deployed in a series of synthetic solutions with different concentrations of P, As, Se, Mo, V and Sb. No evidence of interference from other oxyanions was found, and the competition effects among the oxyanions are

likely to be negligible (Table S15). However, in the presence of oxyanions at lower oxidation states and under varied water conditions, competition effects were observed for oxyanions including V and Se on precipitated ferrihydrite gels and Metsorb gels.[11] Then, possible competition effect among oxyanions of the six oxyanions with different oxidation states in both freshwater and seawater is the subject of further work.

Table S1. Masses of analytes for ICP-MS (PerkinElmer NexION 300X) analysis to characterize laboratory DGT performance. Y and In are chosen as internal standards for analytes from group 1 and 2, respectively.

group	analyte	mass (amu)	corrections	potential interferences
Group 1	V	50.944		ClO, HSO
	As	74.9216		ArCl, Sm++, Nd++, Eu++
	Se	81.9167	-1.007833*Kr83	Kr, BrH, Ar2H, Ho++, Dy++, Er++
	Y	88.9054		
	Mo	97.9055	-0.109613*Ru101	Ru, BrO
Group 2	In	114.904	-0.014038*Sn118	Sn, MoO
	Sb	120.904		

Table S2. Sediment properties.

Sediment property	Value
sediment pH	7.32±0.17
total organic carbon (%, loss on ignition)	4.1±0.3
overlying water temperature (^{o}C)	20±1
particle size (%)	
sand (>50 μm)	4
slit (2-50 μm)	77
clay (<2μm)	19

Table S3. Operating parameters of ICP-MS (7500 Series, Agilent Technologies, USA).

Parameters	value
RF power (W)	1510
RF matching (V)	1.70
Carrier gas (L min^{-1})	1.07
Nebulizer pump (rps)	0.10
S/C temperature (^{o}C)	2

Table S4. Elution efficiencies of P, V, As, Se, Mo and Sb from precipitated zirconia gels eluted using two different eluents. Standard deviations are derived from replicates (n=18).

Eluent	P	V	As	Se	Mo	Sb
A	96.2±1.8%	95.2±1.2%	96.9±1.8%	95.3±5.2%	98.9±1.7%	10.9±1.7%
B	––	98.2±1.0%	92.8±1.0%	91.9±5.0%	97.0±2.5%	100.2±0.8%

A: 10 mL of 0.5 mol L^{-1} NaOH; B: 10 mL of 0.5 mol L^{-1} NaOH/0.5 mol L^{-1} H_2O_2

Table S5. Horizontal shrinkage of each three precipitated zirconia (PZ) and slurry zirconia (SZ) gels discs of circular shape.

	Diameter before gel drying (cm)	Diameter after gel drying (cm)	Area before gel drying (cm^2)	Area after gel drying (cm^2)	Shrinkage %
PZ–1	2.48	2.48	4.83	4.83	0
PZ–2	2.50	2.50	4.91	4.91	0
PZ–3	2.46	2.46	4.75	4.75	0
SZ–1	2.48	2.18	4.83	3.73	22.7
SZ–2	2.48	2.16	4.83	3.66	24.1
SZ–3	2.48	2.18	4.83	3.73	22.7

Table S6. Horizontal shrinkage of each three precipitated zirconia (PZ) and slurry zirconia (SZ) gels discs of quadrangular shape.

	Sides	Length after gel drying (mm)	Length before gel drying (mm)	Area after gel drying (mm^2)	Area before gel drying (mm^2)	Shrinkage %
PZ–1	a1	14.55	14.56			
	b1	15.50	15.50			
	c1	14.81	14.84			
	d1	15.41	15.42	226.87	227.25	0.168
PZ–2	a2	14.89	14.89			
	b2	15.71	15.72			
	c2	15.48	15.48			
	d2	15.37	15.39	235.92	236.15	0.097
PZ–3	a3	14.12	14.12			
	b3	17.08	17.09			
	c3	13.68	13.68			
	d3	17.10	17.10	237.53	237.60	0.029
SZ–1	a4	10.54	14.73			
	b4	13.69	17.98			
	c4	10.98	14.64			
	d4	13.58	17.94	146.69	263.74	44.4
SZ–2	a5	10.97	14.04			
	b5	13.51	17.72			
	c5	11.42	14.12			
	d5	13.00	16.95	148.33	243.98	39.2
SZ–3	a6	10.70	13.97			
	b6	13.39	17.71			
	c6	11.09	14.89			
	d6	13.19	17.42	144.77	253.36	42.9

Table S7. Slope and regression coefficients for the DGT LA-ICP-MS calibration. The slopes are obtained from linear regression of P, As, Mo and Sb fluxes (pg cm^{-2} s^{-1}) versus their measured signals (cps).

Element	Linear slope	R^2
P	6.3058	0.9914
As	3.9401	0.9947
Mo	3.4121	0.9920
Sb	1.7624	0.9912

Table S8. As(III), Se(IV) and Sb(III) uptake efficiencies after immersing precipitated zirconia gel in 10 mL of 100 μg L^{-1} single solutions for 4 h at various pH (4-8) and ionic strength (0.001-0.5 mol L^{-1} $NaNO_3$) range (unit: %). Standard deviations are derived from replicates (n=3).

		As(III)	Se(IV)	Sb(III)
pH	4	98.9±0.1	99.9±0.1	99.7±0.01
	5	98.7±0.4	99.6±0.4	99.3±0.5
	6	98.9±0.2	100±0.1	99.5±0.03
	7	99.1±0.04	99.9%±0.02	99.6±0.07
	8	99.5±0.2	99.7%±0.2	98.6±0.2
ionic strength (unit: mol L^{-1})	0.0001	98.9±0.6	99.7±0.1	99.4±0.3
	0.001	99.2±0.1	99.9±0.03	99.6±0.03
	0.01	99.1±0.01	100±0.01	99.7±0.01
	0.1	98.6±0.9	99.7±0.03	99.6±0.03
	0.5	98.9±0.1	100±0.02	99.6±0.1

Table S9. Pearson correlation coefficients between different elements across the sediment-water interface (SWI) of a freshwater sediment with the depth from 5.0 cm above to 2.0 cm below the SWI (n=2100) and from 2.0 cm below to 14.4 cm below the SWI (n=3660).

	P	As	Mo	Sb
5.0 cm above to 2.0 cm below the SWI, n=2100				
P	1			
As	0.758**	1		
Mo	0.219**	0.239**	1	
Sb	0.251**	0.156**	0.089**	1
2.0 cm below to 14.4 cm below the SWI, n=3660				
P	1			
As	0.398**	1		
Mo	0.258**	0.358**	1	
Sb	0.269**	0.623**	0.257**	1

Level of significance: **$p<0.001$.

Table S10. Fluxes of P, As, Mo and Sb in four discrete zones. The size of each zone is 1200 μm × 3000 μm containing 240 points (see Figure S7), i.e. the standard deviations are derived from 240 replicates. Different superscript letters indicate significant different (Kruskal-Wallis, $p<0.05$, n=240).

Zone	P	As	Mo	Sb
sm	8.94 ± 1.45^{a}	0.59 ± 0.08^{d}	0.024 ± 0.006^{h}	0.015 ± 0.004^{k}
bs	7.74 ± 1.03^{b}	0.32 ± 0.04^{e}	0.018 ± 0.005^{i}	0.007 ± 0.002^{l}
ow	4.63 ± 0.75^{c}	0.43 ± 0.05^{f}	0.016 ± 0.004^{j}	0.003 ± 0.001^{m}
owh	7.73 ± 1.04^{b}	0.70 ± 0.09^{g}	0.019 ± 0.006^{i}	0.005 ± 0.002^{n}

sm= sediment microniche, bs=bulk sediment, ow=overlying water, owh=overlying water hotspot

Table S11. Certified and measured concentrations of V, As, Mo, and Sb [a] in the SLRS-5 river water reference material for trace metals analysis using ICP-MS. Standard deviations are derived from replicates (n=11).

	certified value ($\mu g\ L^{-1}$)	measured value ($\mu g\ L^{-1}$)	Recovery (%)
V	0.317±0.033	0.339±0.098	96.9±6.9
As	0.413±0.039	0.432±0.023	95.7±5.7
Mo	0.5	0.507±0.016	101±10
Sb	0.3	0.308±0.010	103±30

[a] No certified value was established for Se.

Table S12. DGT blanks and DGT method detection limits (MDL=3*standard deviations of blanks) (unit: μg L^{-1}).

	Precipitated zirconia gel blank (MDL)[a]	Slurry ferrihydrite gel blank (MDL)[c]	Precipitated ferrihydrite gel blank (MDL)[c]	Metsorb gel blank (MDL)[d]
P	0.91±0.24 (0.72)[b]	–	0.97±0.22 (0.66)[e]	0.81±0.26 (0.78)[e]
V	0.015±0.007 (0.02)	0.045±0.016 (0.05)	0.015±0.006 (0.02)	0.60±0.11 (0.33)
As	0.046±0.011 (0.03)	0.10±0.053 (0.16)	0.13±0.033 (0.10)	0.29±0.009 (0.03)
Se	0.069±0.022 (0.07)	0.13±0.063 (0.19)	0.063±0.020 (0.06)	–
Mo	0.22±0.029 (0.09)	–	0.100±0.020 (0.06)[d]	0.16±0.022 (0.07)
Sb	0.027±0.004 (0.01)	0.13±0.044 (0.13)	0.026±0.007 (0.02)	0.025±0.006 (0.02)

Note: Gel blank concentrations were calculated using an assumed deployment time of 24 h at 25°C with 0.8 mm thick diffusive gels and 3.14 cm^2 exposure area; a, Eluted with 0.5 mol L^{-1} NaOH/0.5 mol L^{-1} H_2O_2; b, Eluted with 0.5 mol L^{-1} NaOH; c, Gel blanks and MDL reported by Luo et al. [8] using 1 mol L^{-1} HNO_3; d, Gel blanks and MDL reported by Panther et al. [9] (after recalculated using the same D values in this paper) using 1 mol L^{-1} NaOH/1 mol L^{-1} H_2O_2; e, Gel blanks and MDL reported by Panther et al. [12] (after recalculated using the same D values in this paper) using 1 mol L^{-1} NaOH.

Table S13. Elution efficiencies of As and Se from precipitated zirconia gels eluted using different volumes and concentrations of NaOH. Standard deviations are derived from replicates (n=6).

Elutes	As	Se
1 mL of 0.5 mol L^{-1} NaOH	84.5±1.5%	83.5±1.9%
5 mL of 0.5 mol L^{-1} NaOH	93.6±1.5%	92.9±1.7%
10 mL of 0.5 mol L^{-1} NaOH	96.9±3.7%	94.4±1.5%
1 mL of 1.0 mol L^{-1} NaOH	82.7±1.0%	81.6±1.8%
5 mL of 1.0 mol L^{-1} NaOH	93.1±1.4%	90.0±1.5%
10 mL of 1.0 mol L^{-1} NaOH	95.6±2.8%	91.8±1.4%

Table S14. Diffusive coefficients adopted in this study.

	D (E-6 cm^2/sec) at 25^oC
P	6.05[a]
V	8.02±0.35[b]
As	6.78±0.24[b]
Se	7.44±0.09[c]
Mo	6.81±0.28[b]
Sb	6.86±0.30[b]

[a] Zhang et al.[10]
[b] Panther et al.[9]
[c] Bennett et al.[13]

Table S15. The ratio of concentrations of elements measured by DGT containing precipitated zirconia gels to concentrations in solutions with different concentration ratios for P, V, As, Se, Mo and Sb. Standard deviations are derived from replicates (n=3).

Solution	P	V	As	Se	Mo	Sb
1	0.95±0.09	1.04±0.03	0.97±0.04	1.04±0.08	1.04±0.05	1.01±0.03
2	0.96±0.05	1.07±0.03	0.95±0.05	1.00±0.03	1.02±0.06	1.05±0.04
3	1.08±0.11	1.03±0.04	0.99±0.04	0.98±0.03	1.10±0.05	1.01±0.04
4	1.07±0.02	1.03±0.07	0.98±0.07	0.98±0.10	0.99±0.10	1.02±0.07
5	1.08±0.02	0.91±0.03	0.99±0.04	0.87±0.06	1.09±0.05	1.01±0.05

1, P 100 μg L^{-1}, others 500 μg L^{-1}; 2, As 50 μg L^{-1}, others 500 μg L^{-1}; 3, Se 50 μg L^{-1}, others 500 μg L^{-1}; 4, Mo 50 μg L^{-1}, others 500 μg L^{-1}; 5, V, Sb 50 μg L^{-1}, others 5 mg L^{-1}.

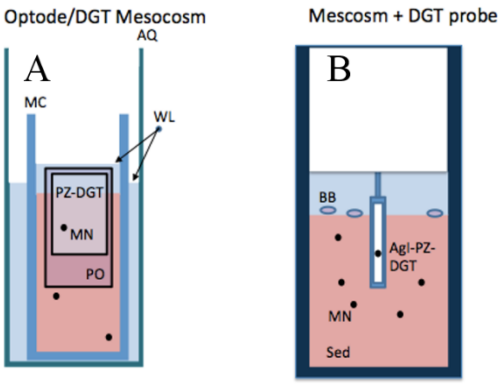

Figure S1. Scheme of the mescosm experimental design. A) Mesocosm. MC = mescocosm, AQ = aquarium, WL = water level, PZ-DGT = precipitated zirconia-DGT, MN = microniche, PO = planar optode. Adapted from Williams et al. 2014.[14] B) Lake deployment. BB = benthic biota (e.g. *Metalita plumulosa*). AgI-PZ-DGT = sulphide gel-percipitation zirconia-DGT, MN = microniche, Sed. = sediment.

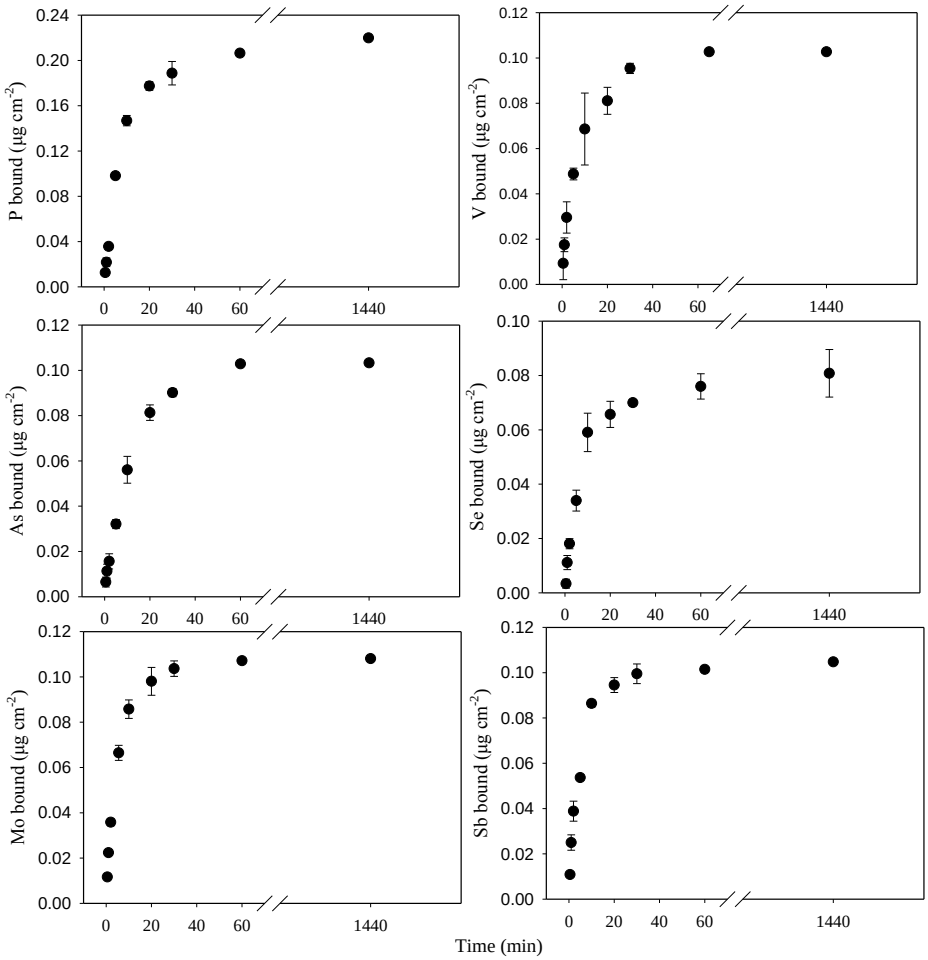

Figure S2. Masses of P, V, As, Se, and Sb bound onto precipitated zirconia gels. The gels were soaked in solutions containing 200 μg L^{-1} P or 100 μg L^{-1} V, As, Se, or Sb for different deployment time. Error bars represent the standard deviations of replicates (n=3).

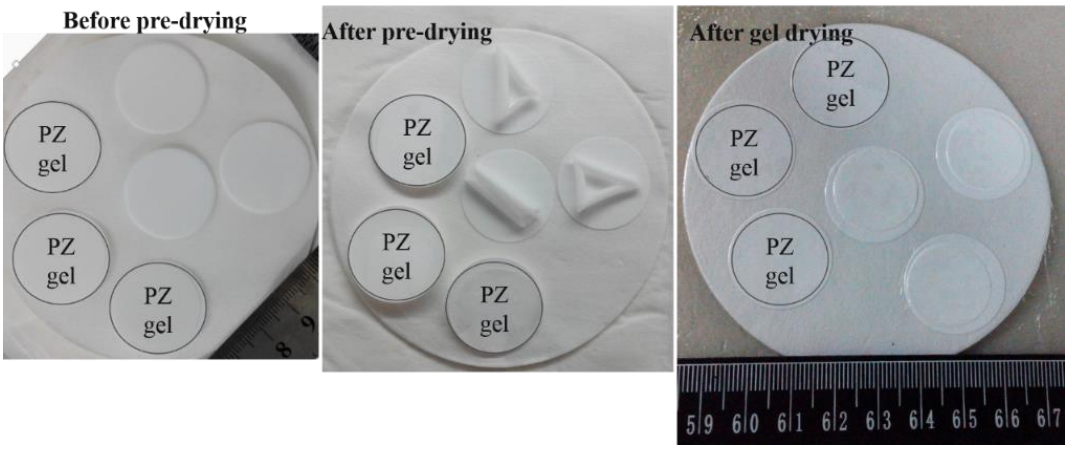

Figure S3. Temporal change of each three precipitated zirconia (PZ) and slurry zirconia (SZ) gels discs of circular shape before and after gel drying. Discs marked PZ gel were PZ gel discs, and the left were SZ gel discs.

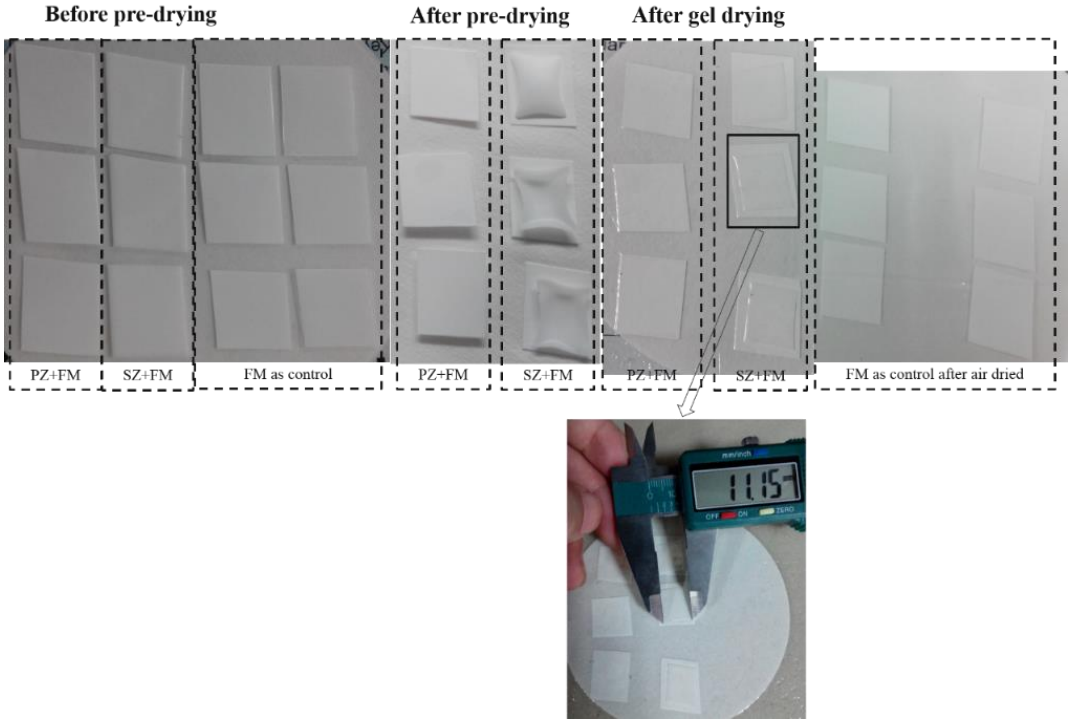

Figure S4. Temporal change of each three precipitated zirconia (PZ) and slurry zirconia (SZ) gels discs of quadrangular shape before and after gel drying. FM represented filter membrane.

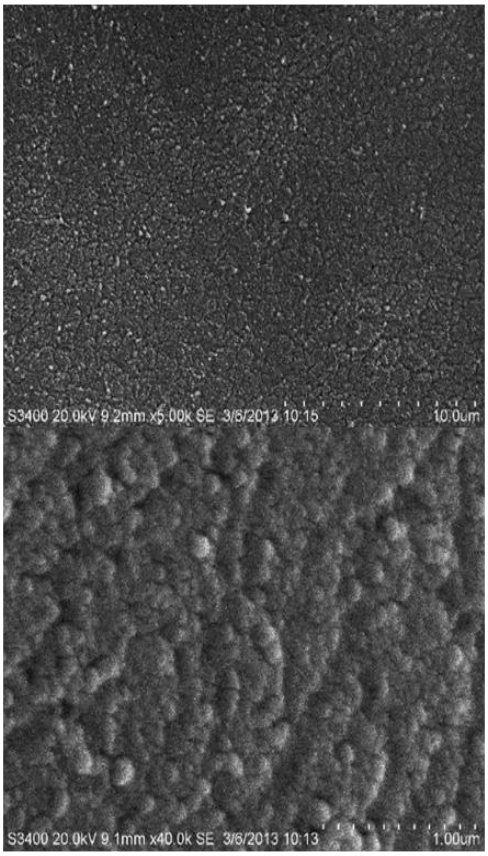

Figure S5. SEM images of precipitated zirconia gel. Scale at 10 μm (up) and 1 μm (down).

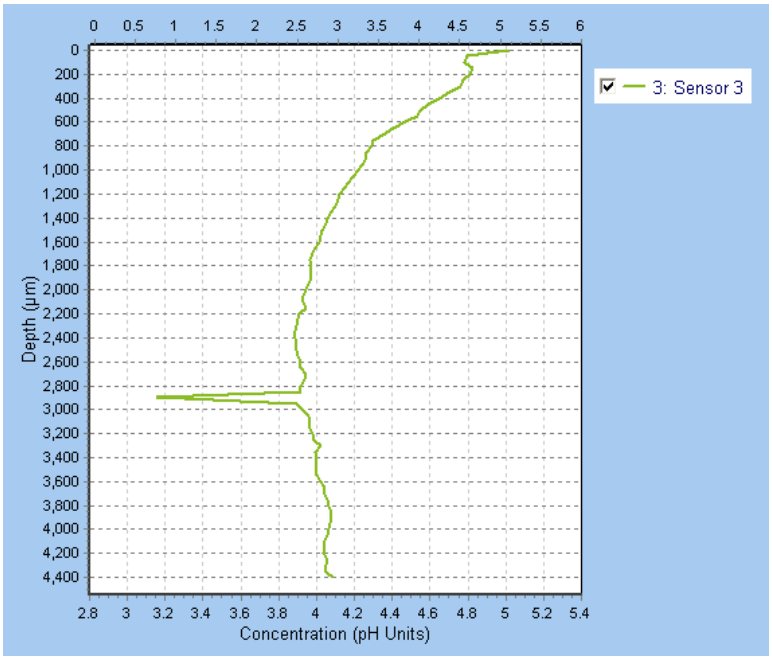

Figure S6. Vertical pH profile in the upper 4.4 mm of the sediment with a resolution of 50 µm.

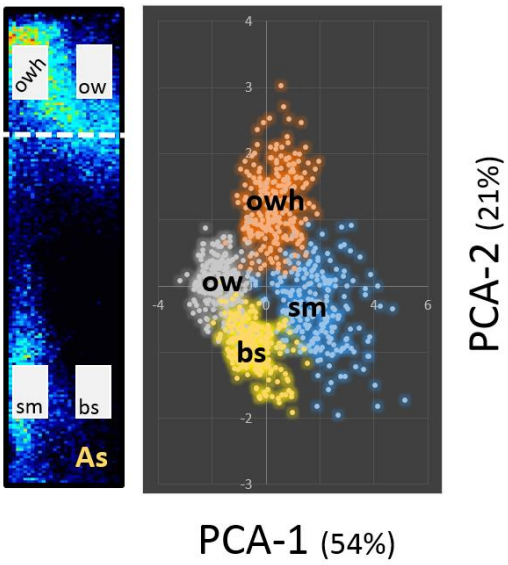

Figure S7. Principal component analysis (PCA) of fluxes of P, As, Mo and Sb in four discrete zones. The size of each zone is 1200 μm × 3000 μm containing 240 points, i.e. n=240.

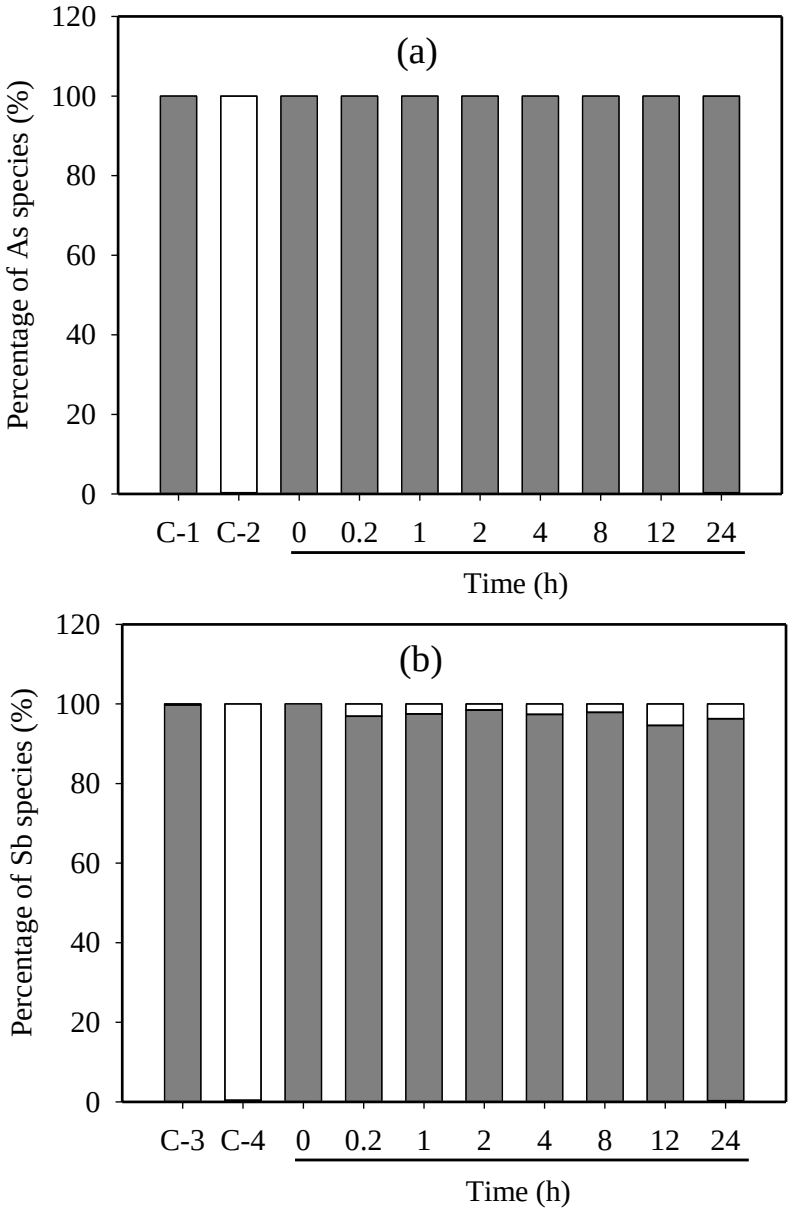

Figure S8. Percentages of As (a) and Sb (b) species during 24 h stirring of 2 L of 100 μg L^{-1} AsIII or SbIII with a matrix of 0.01 mol L^{-1} $NaNO_3$. Solid and open columns represent reduction(III) and oxidation(V) state, respectively, of As and Sb. C-1, C-2, C-3 and C-4 indicate the controls of As and Sb solutions without stirring.

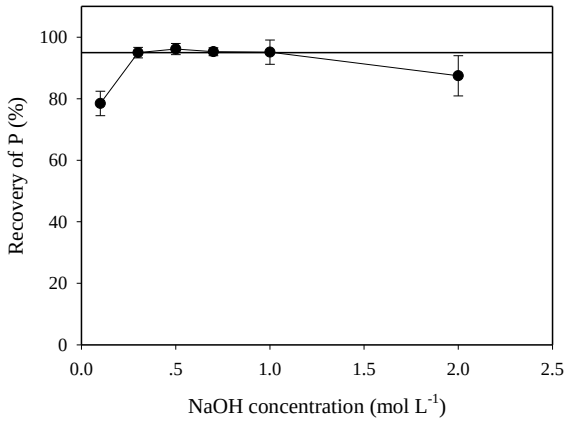

Figure S9. Recovery of P from precipitated zirconia gels eluted using 10 ml of different concentrations of NaOH solution. The solid line shows the 95% recovery of P. Error bars represent the standard deviations of replicates (n=6).

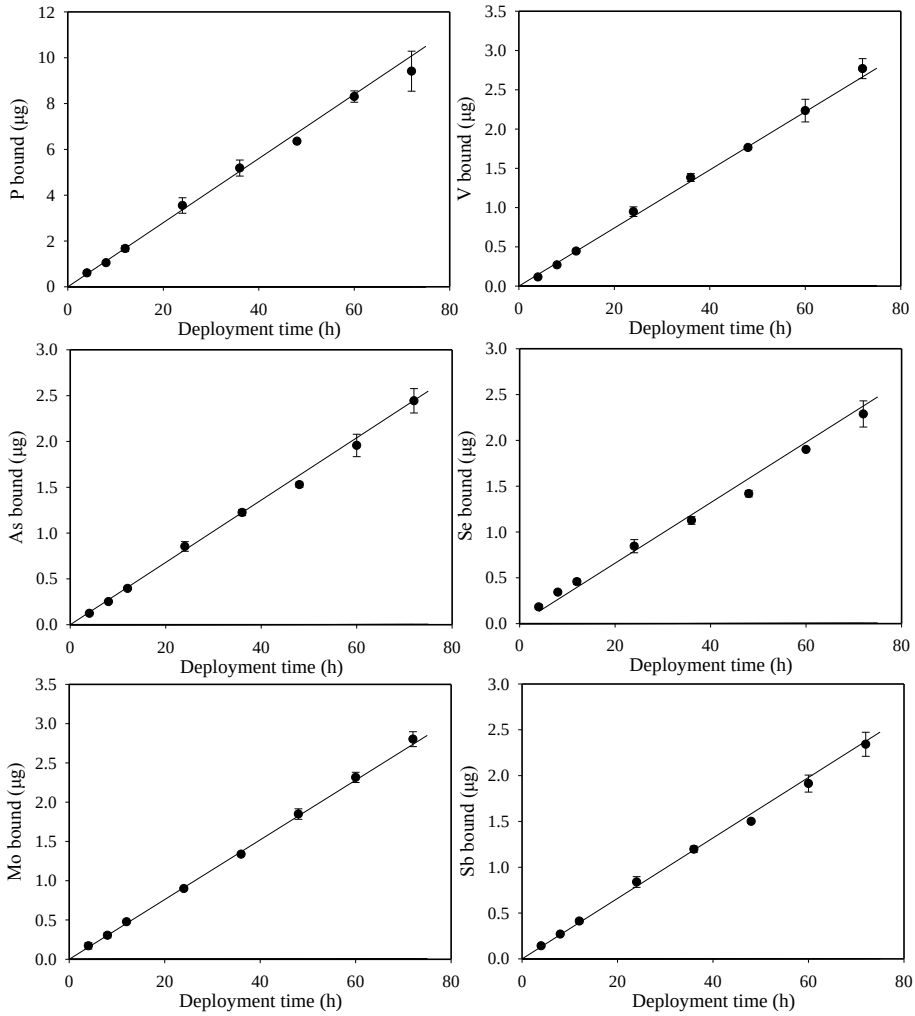

Figure S10. Dependence of measured mass of P, V, As, Se, Mo and Sb accumulated by DGT equipped with precipitated zirconia gels on different deployment time (from 4 to 72 h). The solid lines were calculated from independently measured solution concentrations using equation S4. Error bars represent the standard deviations of replicates (n=3).

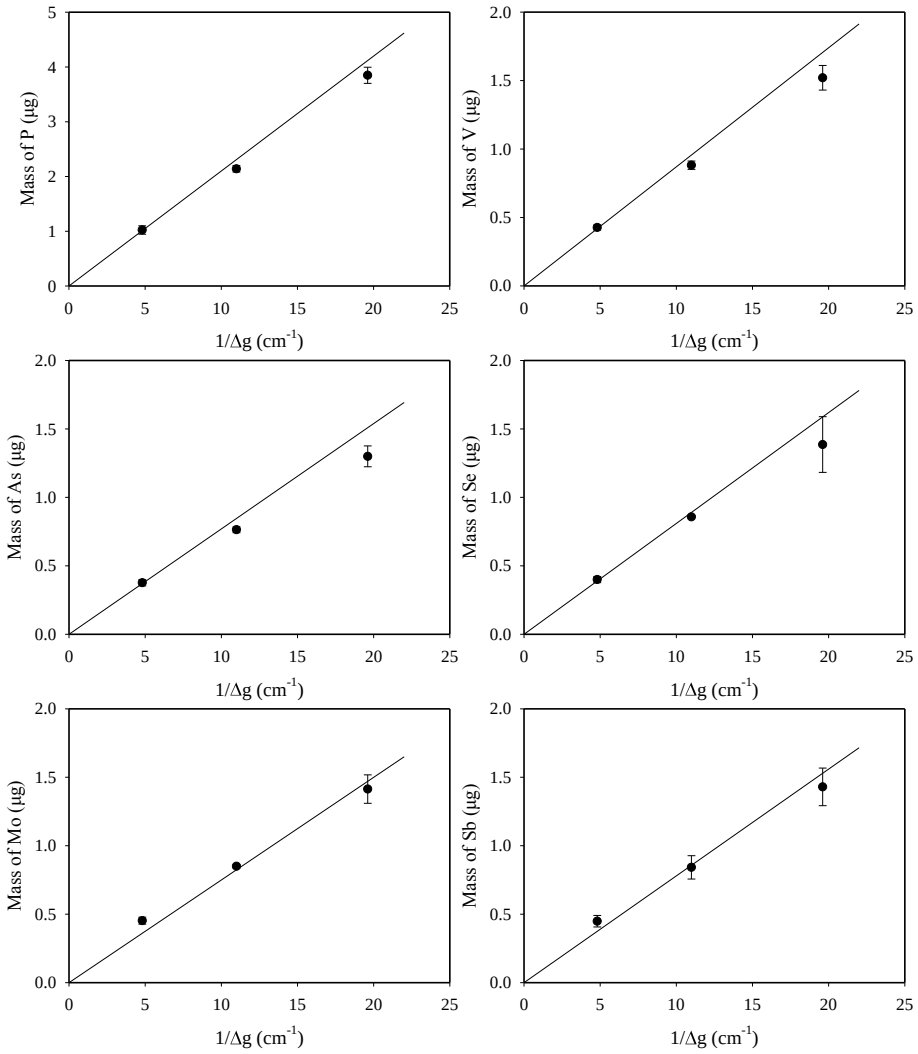

Figure S11. Dependence of the measured mass of P, V, As, Se, Mo and Sb accumulated by DGT devices containing precipitated zirconia gels on the reciprocal of diffusive gel thicknesses (4 h deployment). The solid lines were calculated from independently measured solution concentrations using equation S4. Error bars represent the standard deviations of replicates (n=3).

References

1. Warnken, K. W.; Zhang, H.; Davison, W., Performance characteristics of suspended particulate reagent−iminodiacetate as a binding agent for diffusive gradients in thin films. *Anal. Chim. Acta* **2004,** *508*, (1), 41-51.
2. Zhang, H.; Davison, W., Performance characteristics of diffusion gradients in thin films for the in situ measurement of trace metals in aqueous solution. *Anal. Chem.* **1995,** *67*, (19), 3391-3400.
3. Stockdale, A.; Davison, W.; Zhang, H., 2D simultaneous measurement of the oxyanions of P, V, As, Mo, Sb, W and U. *J. Environ. Monit.* **2010,** *12*, (4), 981-984.
4. Stockdale, A.; Davison, W.; Zhang, H., High−resolution two−dimensional quantitative analysis of phosphorus, vanadium and arsenic, and qualitative analysis of sulfide, in a freshwater sediment. *Environ. Chem.* **2008,** *5*, (2), 143-149.
5. Ding, S.; Jia, F.; Xu, D.; Sun, Q.; Zhang, L.; Fan, C.; Zhang, C., High−resolution, two−dimensional measurement of dissolved reactive phosphorus in sediments using the diffusive gradients in thin films technique in combination with a routine procedure. *Environ. Sci. Technol.* **2011,** *45*, (22), 9680-9686.
6. Ding, S.; Xu, D.; Sun, Q.; Yin, H.; Zhang, C., Measurement of dissolved reactive phosphorus using the diffusive gradients in thin films technique with a high−capacity binding phase. *Environ. Sci. Technol.* **2010,** *44*, (21), 8169-8174.
7. Khaksar, M.; Jolley, D. F.; Sekine, R.; Vasilev, K.; Johannessen, B.; Donner, E.; Lombi, E., In-situ chemical transformations of silver nanoparticles along the water-sediment continuum. *Environ. Sci. Technol.* **2015,** *49*, (1), 318-25.
8. Luo, J.; Zhang, H.; Santner, J.; Davison, W., Performance characteristics of diffusive gradients in thin films equipped with a binding gel layer containing precipitated ferrihydrite for measuring arsenic(V), selenium(VI), vanadium(V), and antimony(V). *Anal. Chem.* **2010,** *82*, (21), 8903-8909.
9. Panther, J. G.; Stewart, R. R.; Teasdale, P. R.; Bennett, W. W.; Welsh, D. T.; Zhao, H., Titanium dioxide−based DGT for measuring dissolved As(V), V(V), Sb(V), Mo(VI) and W(VI) in water. *Talanta* **2013,** *105*, (15), 80-86.
10. Zhang, H.; Davison, W.; Gadi, R.; Kobayashi, T., In situ measurement of dissolved phosphorus in natural waters using DGT. *Anal. Chim. Acta* **1998,** *370*, (1), 29-38.
11. Price, H. L.; Teasdale, P. R.; Jolley, D. F., An evaluation of ferrihydrite- and Metsorb-DGT techniques for measuring oxyanion species (As, Se, V, P): effective capacity, competition and diffusion coefficients. *Anal. Chim. Acta* **2013,** *803*, 56-65.
12. Panther, J. G.; Teasdale, P. R.; Bennett, W. W.; Welsh, D. T.; Zhao, H., Titanium dioxide−based DGT technique for in situ measurement of dissolved reactive phosphorus in fresh and marine waters. *Environ. Sci. Technol.* **2010,** *44*, (24), 9419-9424.
13. Bennett, W. W.; Teasdale, P. R.; Panther, J. G.; Welsh, D. T.; Jolley, D. F., New diffusive gradients in a thin film technique for measuring inorganic arsenic and selenium(IV) using a titanium dioxide based adsorbent. *Anal. Chem.* **2010,** *82*, (17), 7401-7407.
14. Williams, P. N.; Santner, J.; Larsen, M.; Lehto, N. J.; Oburger, E.; Wenzel, W.; Glud, R. N.; Davison, W.; Zhang, H., Localized flux maxima of arsenic, lead, and iron around root apices in flooded lowland rice. *Environ. Sci. Technol.* **2014,** *48*, (15), 8498-8506.